

# Energy Performance of a Reversed Circular Flow Jet Impingement Bifacial Photovoltaic Thermal (PVT) Solar Collector

Muhammad Amir Aziat Ishak<sup>a</sup>

<sup>a</sup> School of Engineering, Faculty of Innovation & Technology, Taylor University, 47500 Subang Jaya, Malaysia

Email: [amir.ishak@taylors.edu.my](mailto:amir.ishak@taylors.edu.my)

**Abstract:** PVT technologies relies on the photovoltaic modules to generate electricity. However, the photovoltaic module itself has a negative downside due to the heat absorbed from being exposed to solar irradiance, resulting in a decline in the module's efficiency. The implementation of a cooling system is important in order to improve its performance. This article presents the energy performance of a bifacial PVT collector cooled by a reversed circular flow jet impingement (RCFJI) by performing indoor experimental. The solar irradiance,  $I$ , tested ranged between 500W/m<sup>2</sup> to 900W/m<sup>2</sup> with a mass flow rate ( $\dot{m}$ ) ranged from 0.01kg to 0.14kg/s. From the analysis, the highest photovoltaic efficiency was observed at  $I = 900\text{W/m}^2$  with 10.91% efficiency. In contrast, the highest thermal and combined photovoltaic thermal performance recorded was 61.4% and 72.35%, respectively under the same operating conditions.

Received 10 February 2025; Accepted 20 May 2025; Available online 30 June 2025

Keywords: Solar collector, Jet impingement, Photovoltaic thermal, Energy analysis, Bifacial

Copyright © 2025 MBOT Publishing.  
All right reserved.

\*Corresponding Author:

Muhammad Amir Aziat Bin Ishak  
School of Engineering,  
Faculty of Innovation & Technology,  
Taylor University, 47500 Subang Jaya, Malaysia  
[amir.ishak@taylors.edu.my](mailto:amir.ishak@taylors.edu.my)

## 1. Introduction

The European Commission's joint research predicted that by 2030, power generation by solar energy would account for more than 10% of global energy consumption (Comello et al., 2018). Solar Energy is a renewable, non-polluting, non-depleting, and unlimited energy source (Yusaidi et al., 2023). Solar energy is more viable than fossil fuels due to its global applicability (Rahmat et al., 2022). There are two categories of direct solar resources (i) solar photovoltaic (PV), which produces electricity from the sunlight; and (ii) solar thermal, generated by harnessing heat from the sun (Bilardo et al., 2020). The incorporation of the two aforementioned technologies is commonly referred to photovoltaic thermal (PVT). Both photovoltaic and thermal are produced simultaneously by the photovoltaic thermal collector (Bassam et al., 2023). The primary benefit of these systems is the reduction in reliance on

non-renewable energy sources (Ishak et al., 2023a). The technology is reliable, with a predicted lifespan of 20-30 years (Ibrahim et al., 2011).

Despite the wide range of advantages, the PVT technology also has a negative drawback: it gains heat from sun exposure, which indirectly decreases the PV efficiency (Rahmat et al., 2022). There are two primary categories of photovoltaic modules: mono-facial and bifacial modules (Ma et al., 2022). Compared to mono-facial modules, a bifacial PV module has the potential to exhibit excellent characteristics. More electricity can be generated as both sides of the PV module are utilized to absorb sunlight (Ishak et al., 2023d). However, cooling alternatives available for bifacial modules are more limited compared to monofacial modules due to the critical role of both sides of the module. While monofacial modules can employ cooling techniques such as fins, cooling coils, and phase change materials, these

approaches are not as feasible for bifacial PV modules. (Ooshaksaraei et al., 2017). Heat transmission in jet impingement is a topic of substantial study which is a reliable approach to enhance heat transfer for bifacial solar collectors (Choo et al., 2016).

This article presents the energy performance of a bifacial PVT collector cooled by a reversed circular flow jet impingement (RCFJI) by performing indoor experimental. The RCFJI works to circulate the airflow inside the cup and leaves the 3mm diameter jet holes outlet with a significant increase in airspeed while impinges the bifacial module. Consequently, enhancing the heat transfer which contributes to improved energy performance (Ishak et al., 2023c). Based on a literature review carried out by Amir et al. (2023), this study is

classified as jet impingement under the jet plate method, as presented in Fig. 1 (Ishak et al., 2023b). Several statements from previous studies could bolster this study. According to Gu et al. (2022), bifacial solar technologies have reached a mature stage. However, further study is necessary to enhance their performance (Ma et al., 2022). Ewe et al. (2021) highlight a lack of scholarly investigations pertaining to the utilization of bifacial modules employing jet impingement (Ewe et al., 2021). Poorya et al. (2017) stated that additional research is necessary to improve a bifacial module's efficacy (Ooshaksaraei et al., 2017). This study fills the research gap by presenting a novel cooling approach incorporating jet impingement application and a method to enhance a bifacial module solar collector.

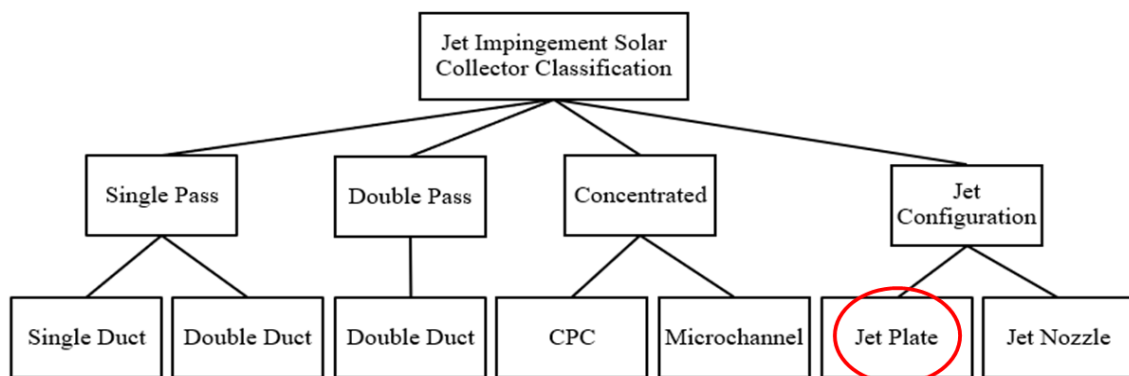


Figure. 1 Jet impingement classification in solar collector applications (Ishak et al., 2023b).

## 2. Methodology

### 2.1 Experimental Procedure

An indoor experiment has been carried using a solar simulator as presented in Fig. 2, to evaluate and analyze the energy performance of the Novel Circular Flow Jet Impingement on a Bifacial Photovoltaic Thermal PVT Solar Collector. In order to replicate the effects of artificial solar irradiance, the solar simulator is outfitted with 32 tungsten halogen lamps, each capable of producing 500 Watts. 14 K-type thermocouples connected to an AT4824 Data logger were calibrated before placing it around the RCFJI PVT solar collector to measure the temperature. The calibration was done by immersing the thermocouple probes in boiling water to ensure that all the thermocouples produced uniform readings across the board. The procedure was carried out using a framework developed from previous research (Ooshaksaraei et al., 2017) (Moshery et al., 2021).

The experiment was performed utilizing a high-velocity airflow generated by an air compressor is required to achieve optimal heat transfer. The air compressor velocity that serves as the air inlet is set to m varying from 0.01kg/s to 0.14kg/s. Furthermore, a pyranometer is used to measure and adjust the solar simulator to a solar radiance level from 500W/m<sup>2</sup> to 900W/m<sup>2</sup>. Thermocouples were connected to the data logger to record the collector's temperature at every 1-second time period for 30 minutes. It was observed that an absence of notable temperature variations was evident as the PVT collector attained a condition of equilibrium within a time frame of roughly 25-30 minutes. Within 10 minutes of steady state, the data from the I-V tracing device was imported into Microsoft Excel, and the I-V properties were plotted. After the completion of data collection, a cooling period of two hours was observed for the collector prior to commencing a further experiment on operating parameters.



Figure. 2 Experiment setup.

## 2.2 Components of RCFJI Bifacial PVT Collector

The photovoltaic panel consists of a bifacial module with a packing factor of 0.66. The packing factor refers to the area covered by the bifacial cells on a PV module, affecting both module's output power and the temperature at which it can operate. Bifacial cells have a significant advantage over traditional photovoltaics and mono-facial modules by absorbing sunlight through both front and rear surfaces of the module. The bifacial module was positioned above the jet plate with a reflectivity of  $n_R$  of 0.17. The characteristic of the bifacial module is presented in Table 1. The RCFJI Bifacial PVT collector was made from a 4mm composite panel filled with thermal insulation foam. The reversed circular flow jet impingement was placed beneath the solar module allowing an air duct of 25mm for heat transfer. An air compressor was used to distribute air to the RCFJI cup through a 6mm polyurethane tube, producing a circular flow inside the cup. Subsequently, the air exits through the 3mm diameter jet holes outlet with high speed and impinges the bifacial modules.

Table 1. Bifacial module characteristic.

Parameters	Value
Packing factor	0.66
Rated maximum power	60W
Voltage at maximum power	17.14V
Current at maximum power	3.5A
Open circuit voltage	22.1V
Short circuit current	3.71A

The reversed circular flow cup was fabricated through 3D printing using polylactic Acid (PLA) filament, as shown in Fig. 3. PLA filament can withstand temperatures up to 110°C without becoming brittle and has a melting point higher than 150°C. The RCFJI was mounted beneath a jet plate consisting of 36 jet holes

outlet, each of the sizes of 3mm, while the streamwise and spanwise values were 113.4mm and 126mm, respectively. A 6mm polyurethane tube was fitted at each reversed circular flow cup inlet to distribute air via jet plate throughout the PVT system. Compressed air will be distributed through a 6mm polyurethane tube fitted on the reversed circular flow cup to produce circular flow before leaving the 3mm diameter jet holes at high speed and impinges the bifacial module.

## 3. Energy Analysis

Energy analysis was performed on the Reversed circular flow jet impingement bifacial PVT solar collector. The parameters and values used in the energy analysis can be referred to in Table 2.

Table 2. Parameters and values.

Parameter	Value
Mass flow rate, $\dot{m}$	0.1 – 0.14 kg/s
Width of collector, W	0684mm
Length of collector, L	705mm
Duct Depth, d	25mm
Solar irradiance, I	500, 600, 700, 800, 900 W/m <sup>2</sup>
Area of collector, $A_c$	0.48 m <sup>2</sup>
Temperature ambient, $T_a$	30 °C
Absorptivity of PV cell, $\alpha_{pv}$	0.91
Packing factor, P	0.66
Heat transfer coefficient, h	9 W/(m <sup>2</sup> .K)
External temperature, $T_{ext}$	30 °C
Transmittance of Lamination, $T_l$	0.85
Reflectivity of jet plate, $n_R$	0.7
Electrical efficiency at reference condition, $\eta_{ref}$	0.16
Temperature Coefficient, $\beta$	0.0045 K <sup>-1</sup>
Temperature at reference condition, $T_{ref}$	303.15 K

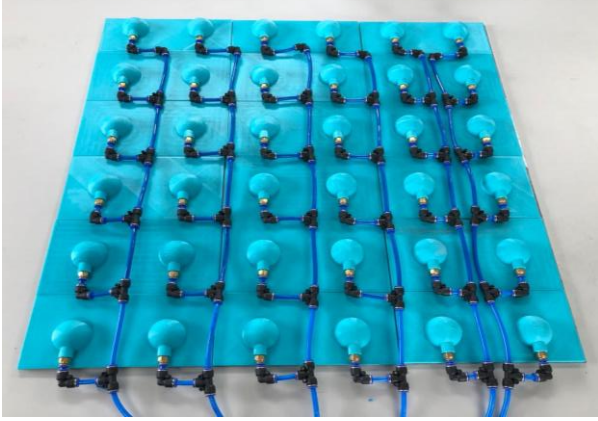


Figure. 3 Fully assembled RCFJI equipped with 6mm air hose.

### 3.1. Reynolds Number

Reynolds number was calculated using the following expression to ascertain the flow characteristic of the system [16];

$$\text{Reynolds number} = \frac{\dot{m}Dh}{Wd\mu} \quad (1)$$

Which hydraulic diameter, Dh, is determined using [16]:

$$Dh = \frac{4Wd}{2(W+d)} \quad (2)$$

While air viscosity,  $\mu$  is determined by [16]:

$$\mu = [1.983 + 0.00184(T - 300)] \times 10^{-5} \quad (3)$$

### 3.2. Convective Heat Flux

Where convective heat flux,  $q_0$ , can be calculated as:

$$q_0 = h.(T_{ext} - T_{PV}) \quad (4)$$

### 3.3. Photovoltaic Efficiency

The photovoltaic efficiency,  $\eta_{\text{photovoltaic}}$ , can be computed as:

$$\eta_{\text{photovoltaic}} = \frac{P_{\text{max}}}{(I \times A_c)} \quad (5)$$

$P_{\text{max}}$  is determined using an I-V tracer which can also theoretically expressed as follows [17]:

$$P_{\text{max}} = IA_c\alpha_{PV}P(\eta_{PV\text{front}}) + IA_cT_i(1 - P)n_r\alpha_{PV}P(\eta_{PV\text{rear}}) \quad (6)$$

The efficiency of the cell is expressed as [17]:

$$\eta_{PV\text{front}} = \eta_{PV\text{rear}} = \eta_{\text{ref}}[1 - \beta(T_{PV} - T_{\text{ref}})] \quad (7)$$

### 3.4. Thermal Efficiency

The thermal efficiency,  $\eta_{\text{thermal}}$  is given as follows [18]:

$$\eta_{\text{thermal}} = \frac{Qu}{(I \times A_c)} \quad (8)$$

The useful heat gain,  $Qu$ , is expressed as:

$$Qu = \dot{m}C_p(T_{\text{out}} - T_{\text{in}}) \quad (9)$$

The temperature (Kelvin) linearly affects the physical properties [19]. Where the specific heat capacity of air,  $C_p$ , can be expressed as:

$$C_p = 1.0057 + 0.000066(T - 300) \quad (10)$$

### 3.5. Combined Photovoltaic Thermal Efficiency (PVT)

The combined PVT efficiency of the PVT collector was calculated using the following equations:

$$\eta_{PVT} = \eta_{\text{photovoltaic}} + \eta_{\text{thermal}} \quad (11)$$

### 3.6. Uncertainty Analysis

Uncertainty analysis is a method used to quantify estimation errors systematically. Inaccuracies in the measurements cast doubt on the reliability of the data. Uncertainty analysis was performed on each measuring equipment to assess the level of uncertainty, as shown in Table 3. 10 sets of readings were taken for every set of measuring equipment. It was observed that the score is approximately 70-90% showing similar traits. Overall, the uncertainty analysis was lower than 2%, indicating that the measurement is precise. The uncertainty results demonstrated that the experiment was reliable. The standard deviation,  $s$  can be calculated by:

$$s = \sqrt{\frac{\sum_i^n (x_i - \bar{x})^2}{n-1}} \quad (12)$$

While the uncertainty is determined by:

$$u = \frac{s}{\sqrt{n}} \quad (13)$$

Table 3. Measurement equipment uncertainty.

Device	Brand	Attributes	Unit	Uncertainty (%)
I-V tracing	MP-11	Solar irradiance	W/m <sup>2</sup>	± 0.65%
Data Logger	AT4824	Temperature	°C	± 0.1 °C
Thermocouples	K-type	Temperature	°C	± 0.1 °C
Pyranometer	TES132	Solar irradiance	W/m <sup>2</sup>	± 1.3%
Anemometer	MT-4615	Air velocity	m/s	± 1.45%

#### 4. Results and Discussions

##### 4.1. Photovoltaic Efficiency

Based on the results presented in Fig. 4, a noticeable decrease in the bifacial module's temperature can be observed in increase. Increasing the  $\dot{m}$  is associated with a greater heat transfer, which subsequently results in enhanced photovoltaic efficiency. Lowering the solar irradiance will decrease the bifacial module's temperature due to less heat being gained. The correlation between photovoltaic efficiency and module temperature is directly proportional. Increasing the solar irradiance will cause the bifacial module's temperature to increase due to heat uptake. In return, this causes the bifacial module to operate at a hotter temperature, which reduces its ability to produce usable electricity. Hence, lowering the collector's temperature is imperative to enhance photovoltaic efficiency. At incident  $I = 900\text{W/m}^2$ , the temperature of the photovoltaic module varies between  $44.3^\circ\text{C}$  to  $55.2^\circ\text{C}$ , while the corresponding photovoltaic efficiency varies between  $10.18\%$  to  $10.91\%$ . Meanwhile, when operating at  $I = 500\text{W/m}^2$ , the bifacial module's temperature varies within the range of  $36.3^\circ\text{C}$  to  $44.6^\circ\text{C}$ , while the photovoltaic efficiency varies between  $10.80\%$  to  $11.38\%$ . Overall, it was observed that the highest  $\eta_{pv}$  obtained was  $11.38\%$  at  $I = 500\text{W/m}^2$  solar irradiance. Conversely, when exposed to  $I = 900\text{W/m}^2$ , the maximum  $\eta_{pv}$  efficiency was  $10.91\%$ .

Fig. 5 presents the current, (I) - voltage, (V) properties across varying irradiance levels at  $\dot{m} = 0.14\text{kg/s}$ . The maximum voltage was attained at  $I = 900\text{W/m}^2$ . In general, there exists a correlation between the voltage and the bifacial module temperature, whereas the current is correlated to the solar irradiance. Meanwhile, the minimum voltage reading was measured at an intensity of  $I = 500\text{W/m}^2$ . Overall, the highest voltage reading observed was  $19.86\text{V}$ , while the highest current was  $3.54\text{A}$  at  $I = 900\text{W/m}^2$ . On the other hand, at  $I = 500\text{W/m}^2$ , the highest voltage obtained was  $15\text{V}$ ,

while the highest current was  $2.47\text{A}$ . In addition, the power (P) – voltage (V) properties showed a positive correlation exists between the solar irradiance and the module's power, as presented in Fig 5. The bifacial module's power exhibits a reduction when subjected to lower irradiance levels.

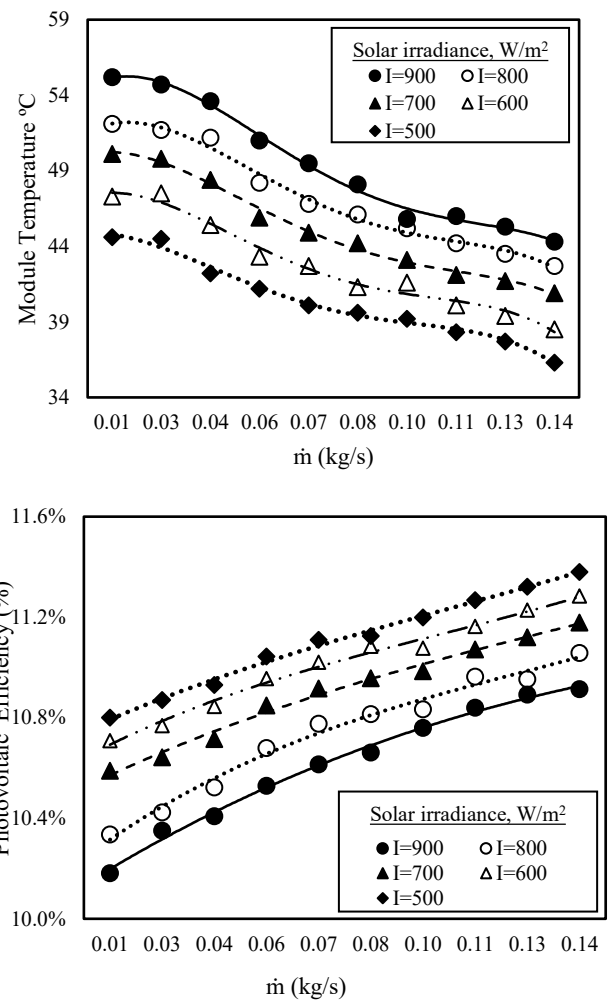


Figure. 4 Module temperature and photovoltaic efficiency at varying irradiance levels.

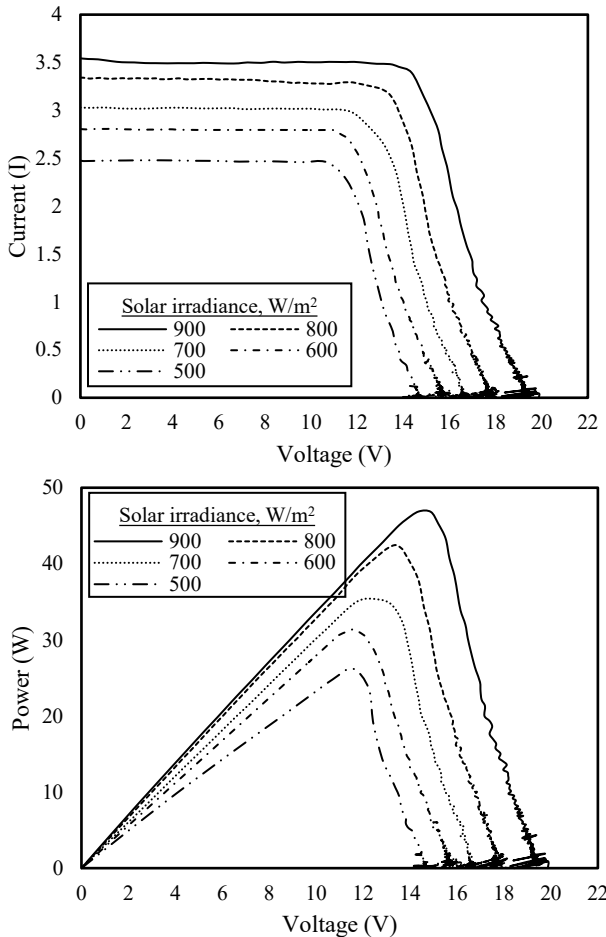


Figure. 5 Current VS voltage and power VS voltage properties curve.

#### 4.2. Thermal Efficiency

When solar irradiance increases, the solar collector absorbs more heat, leading to a rise in the PVT solar collector outlet temperature, as illustrated in Fig 6. This, in turn, results in a higher the thermal efficiency. The thermal efficiency and output temperature is directly proportional, while the correlation between the thermal efficiency and solar irradiance is inversely proportional. When the outlet temperature rises, the thermal efficiency increases. At the maximum tested irradiance of  $900\text{W/m}^2$ , the temperature at the outlet falls within the range of  $35.13\text{--}43.93^\circ\text{C}$ , while the corresponding  $\eta_{th}$  ranges from  $34.5\text{--}61.4\%$ . at the lowest irradiance of  $500\text{W/m}^2$ , the output temperature falls within the range of  $31.33\text{--}35.49^\circ\text{C}$ , while the  $\eta_{th}$  varies between  $31.3\text{--}54.3\%$ . Overall, the highest outlet temperature recorded was  $43.93^\circ\text{C}$ , which was attained at an incident  $I = 900\text{W/m}^2$  and  $\dot{m} = 0.14\text{kg/s}$ . The  $\eta_{th}$  demonstrates an observable improvement with an increase in the  $\dot{m}$ , mainly due to the enhanced airflow circulation inside the collector. In addition, the highest  $\eta_{th}$  recorded was  $61.4\%$  at  $I = 900\text{W/m}^2$  and  $\dot{m} = 0.14\text{kg/s}$ .

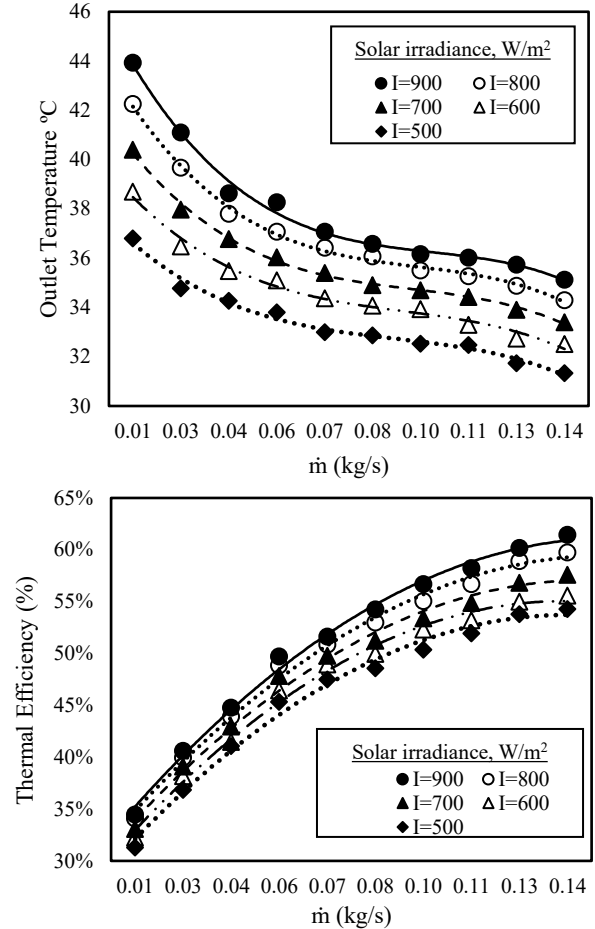


Figure. 6 Outlet temperature and thermal efficiency at varying irradiance levels.

#### 4.3. Combined Photovoltaic Thermal Efficiency (PVT)

According to Fig. 7, the greatest combined PVT efficiency attained was at  $I = 900\text{W/m}^2$ , with  $\eta_{pv}$  of  $10.91\%$  and  $\eta_{th}$  of  $61.43\%$ , respectively. Hence, the aggregate  $\eta_{PVT}$  was  $72.35\%$  at  $I = 900\text{W/m}^2$ . Meanwhile, at  $I = 500\text{W/m}^2$ , the highest  $\eta_{pv}$ ,  $\eta_{th}$ , and  $\eta_{PVT}$  was  $11.38\%$ ,  $54.28\%$ , and  $65.66\%$ . It was observed that the combined PVT efficiency increases as mass flow rate increases due to more energy is produced.



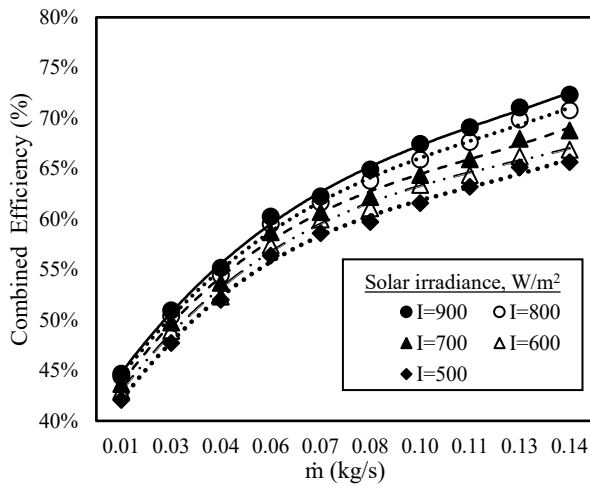


Figure. 7 Combined PVT efficiency at varying irradiance levels.

### 5. Conclusion

This article presents the energy performance of a bifacial PVT collector cooled by a reversed circular flow jet impingement (RCFJI) by performing indoor experimental. The RCFJI bifacial PVT was tested with  $I = 500\text{W/m}^2$  to  $900\text{W/m}^2$  with  $\dot{m}$  varying from  $0.01\text{kg/s}$  to  $0.14\text{kg/s}$ . The results indicated that the PVT collector's photovoltaic performance achieved its highest efficiency when exposed to an irradiance level of  $500\text{W/m}^2$  and  $\dot{m} = 0.14\text{ kg/s}$  with  $11.38\%$  efficiency. When operating at  $I = 900\text{W/m}^2$ , the RCFJI bifacial PVT collector attained  $\eta_{pv}$  of  $10.91\%$ . In addition, the highest  $\eta_{th}$  attained was  $61.4\%$  when subjected to a  $I = 900\text{W/m}^2$  and  $\dot{m} = 0.14\text{ kg/s}$ . The  $\eta_{th}$  reached its lowest value at  $54.28\%$  when the incident was subjected to  $I = 500\text{W/m}^2$  and  $\dot{m}=0.14\text{ kg/s}$ . The greatest combined PVT efficiency was  $72.35\%$  at  $I = 900\text{ W/m}^2$ . In contrast, the lowest PVT efficiency was obtained at  $I = 500\text{W/m}^2$  was  $65.66\%$ . The results obtained showed energy performance improved due to the RCFJI, which promotes circular flow in the circular cup. The airflow then leaves the jet holes with high speed while impinges the bifacial module. Simultaneously, enhancing the heat transfer rate inside the. The swirling effect from the circular flow promotes turbulent flow and prevents the boundary layer development, which improves heat transfer. Based on the current ( $I$ ) – voltage ( $V$ ) properties shown in Fig. 5, it was observed that there was a noise in the curve caused by a shadow underneath the bifacial module. Thus, a compound parabolic concentrator (CPC) is recommended beneath the bifacial module to allow better light reflection and overcome the shadow.

Nomenclature			
Ac	Area of collector	Greek	
d	Duct depth	$\alpha_{pv}$	Absorptivity of PV cell
h	Heat transfer coefficient	$\beta$	Temperature Coefficient
I	Solar irradiance	n	Sets of measurement
L	Length of collector	$\dot{m}$	Mass flow rate
P	Packing factor	$\eta_{pv}$	Photovoltaic efficiency
PLA	polylactic Acid	$n_R$	Reflectivity of jet plate
PV	Photovoltaic	$n_{ref}$	Electrical efficiency at reference condition
PVT	Photovoltaic thermal	$\eta_{th}$	Thermal efficiency
RCFJI	Reversed circular flow jet impingement	$\eta_{PVT}$	Photovoltaic thermal efficiency
Ta	Temperature ambient	$\tau_l$	Transmittance of Lamination
W	Width of collector	$T_{ref}$	Temperature at reference condition
		$\bar{x}_i$	Mean of measurement
		$\bar{x}$	Measurement results

### References

Bassam, Abdulsahib M., Sopian, Kamaruzzaman, Ibrahim, Adnan, Fauzan, Mohd Faizal, Al-Aasam, Anwer B., & Abusaibaa, Ghaith Yahay. (2023). Experimental analysis for the photovoltaic thermal collector (PVT) with nano PCM and micro-fins tube nanofluid. *Case Studies in Thermal Engineering*, 41(November 2022). <https://doi.org/10.1016/j.csite.2022.102579>

Bilardo, Matteo, Ferrara, Maria, & Fabrizio, Enrico. (2020). Performance assessment and optimization of a solar cooling system to satisfy renewable energy ratio (RER) requirements in multi-family buildings. *Renewable Energy*, 155, 990–1008. <https://doi.org/10.1016/j.renene.2020.03.044>

Choo, Kyosung, Friedrich, Brian K., Glaspell, Aspen W., & Schilling, Karen A. (2016). The influence of nozzle-to-plate spacing on heat transfer and fluid flow of submerged jet impingement. *International Journal of Heat and Mass Transfer*, 97, 66–69. <https://doi.org/10.1016/j.ijheatmasstransfer.2016.01.060>

Comello, Stephen, Reichelstein, Stefan, & Sahoo, Anshuman. (2018). The road ahead for solar PV power. *Renewable and Sustainable Energy Reviews*, 92(May), 744–756. <https://doi.org/10.1016/j.rser.2018.04.098>

Ewe, Win Eng., Fudholi, Ahmad., Sopian, Kamaruzzaman., Asim, Nilofar., Ahmudiarto,

- Yoyon., & Salim, Agus. (2021). Overview on Recent PVT Systems with Jet Impingement. *International Journal of Heat and Technology*, 39(6), 1951–1956. <https://doi.org/10.18280/ijht.390633>
- Ibrahim, Adnan, Othman, Mohd Yusof, Ruslan, Mohd Hafidz, Mat, Sohif, & Sopian, Kamaruzzaman. (2011). Recent advances in flat plate photovoltaic/thermal (PV/T) solar collectors. *Renewable and Sustainable Energy Reviews*, 15(1), 352–365. <https://doi.org/10.1016/j.rser.2010.09.024>
- Ishak, Muhammad Amir Aziat Bin., Ibrahim, Adnan., Fazlizan, Ahmad., Fauzan, Mohd Faizal., Sopian, Kamaruzzaman., & Rahmat, Muhammad Aqil Afham. (2023a). Exergy performance of a reversed circular flow jet impingement bifacial photovoltaic thermal (PVT) solar collector. *Case Studies in Thermal Engineering*, 49. <https://doi.org/10.1016/j.csite.2023.103322>
- Ishak, Muhammad Amir Aziat Bin., Ibrahim, Adnan., Sopian, Kamaruzzaman., Fauzan, Mohd Faizal., Rahmat, Muhammad Aqil Afham., & Hamid, Ag sufiyan Abd. (2023b). Classification of Jet Impingement Solar Collectors – A Recent Development in Solar Energy Technology. *International Journal of Renewable Energy Research-IJRER*, 13(2), 802–817. <https://doi.org/https://doi.org/10.20508/ijrer.v13i2.13884.g8755>
- Ishak, Muhammad Amir Aziat Bin., Ibrahim, Adnan., Sopian, Kamaruzzaman., Fauzan, Mohd Faizal., Rahmat, Muhammad Aqil Afham., & Hamid, Ag sufiyan Abd. (2023c). *Heat Transfer Performance of a Novel Circular Flow Jet Impingement Bifacial Photovoltaic Thermal PVT Solar Collector*. 13(2). <https://doi.org/https://doi.org/10.20508/ijrer.v13i2.13886.g8756>
- Ishak, Muhammad Amir Aziat Bin., Ibrahim, Adnan., Sopian, Kamaruzzaman., Fauzan, Mohd Faizal., Rahmat, Muhammad Aqil Afham., & Yusaidi, Nurul Jannah. (2023d). Performance and Economic Analysis of a Reversed Circular Flow Jet Impingement Bifacial PVT Solar Collector. *International Journal of Renewable Energy Development*, 12(4), 780–788. <https://doi.org/https://doi.org/10.14710/ijred.2023.54348>
- Ma, Tao, Kazemian, Arash, Habibollahzade, Ali, Salari, Ali, Gu, Wenbo, & Peng, Jinqing. (2022). A comparative study on bifacial photovoltaic/thermal modules with various cooling methods. *Energy Conversion and Management*, 263(February), 115555. <https://doi.org/10.1016/j.enconman.2022.115555>
- Moshery, Refat, Chai, Tan Yong, Sopian, Kamaruzzaman, Fudholi, Ahmad, & Al-Waeli, Ali H. A. (2021). Thermal performance of jet-impingement solar air heater with transverse ribs absorber plate. *Solar Energy*, 214(December 2020), 355–366. <https://doi.org/10.1016/j.solener.2020.11.059>
- Ooshaksaraei, Poorya, Sopian, Kamaruzzaman, Zaidi, Saleem H., & Zulkifli, Rozli. (2017). Performance of four air-based photovoltaic thermal collectors configurations with bifacial solar cells. *Renewable Energy*, 102, 279–293. <https://doi.org/10.1016/j.renene.2016.10.043>
- Rahmat, Muhammad Aqil Afham., Hamid, Ag Sufiyan Abd., Lu, Yuanshen., Ishak, Muhammad Amir Aziat Bin., Suheel, Shaikh Zishan., Fazlizan, Ahmad., & Ibrahim, Adnan. (2022). An Analysis of Renewable Energy Technology Integration Investments in Malaysia Using HOMER Pro. *Sustainability (Switzerland)*, 14(20). <https://doi.org/10.3390/su142013684>
- Yusaidi, Nurul Jannah, Fauzan, Mohd Faizal, Ibrahim, Adnan, Jarimi, Hasila, Fazlizan, Ahmad, & Sopian, Kamaruzzaman. (2023). Recent development on double pass solar thermal collector. *Renewable and Sustainable Energy Reviews*, 183(June), 113545. <https://doi.org/10.1016/j.rser.2023.113545>